Egypt. J. Chem. **Vol. 65,** No. 10 pp. 551 - 559 (2022)

Egyptian Journal of Chemistry

http://ejchem.journals.ekb.eg/

Synthesis and Photocatalytic Activity of TiO_2-coupled SnO_2 Nanoparticles Prepared By Sol–Gel Technique

Fadhela M.Hussein, Yousif K. Abdul Amir, Ramzei R. AL-Ani, Ali MA. AL-Mokaram*

[1]*Department of Chemistry, College of Science, Mustansiriyha University, Baghdad, 10052, Iraq*

[2]*Al-Turath University College , Baghdad. Iraq.*

[3]*Alnukhba University college , Baghdad , Iraq.*

Abstract

Sol–gel technique was applied to synthesis TiO_2 with SnO_2 nanoparticles in relatively acidic media. X-ray diffraction measurements showed that TiO_2/SnO_2 nanoparticles were polycrystalline at the anatase phase. TiO_2/SnO_2 nanoparticles were examined using atomic force microscopy, scanning electron microscopy and Fourier transform infrared analysis. The band gap for the TiO_2/ SnO_2 nanoparticle estimated from UV–vis spectroscopy was 3.69 eV and also varied in order to investigate the effects of these parameter such as nanoparticle loading, pH, initial p-NT concentration, and temperature, on the reaction kinetics. The TiO_2-coupled SnO_2 nanoparticles in general showed higher photocatalytic activities than the pure ones. Kinetic studies that the reaction is pseudo first order, and the rate of reaction decreased with increasing p-Nitrotoluene initial concentration, and the used different light source showed the visible light was most Efficiency.

Keywords:Sol–gel technique, X-ray diffraction, Polycrystalline, UV–vis spectroscopy, p-nitrotoluene

1. Introduction

Semiconductor nanoparticles have gained considerable attention because of their potential applications in sunlight-based vitality transformation [1, 2], heterogeneous photo catalysis [3] and dielectrics [4]. Several semiconductor nanoparticles, such as SnO_2, ZnO, WO_3 and Fe_2O_3, have been utilized for the previously mentioned applications. However, TiO_2 is the most high-potential material among the recently identified materials because of its excellent optical properties, such as a high refractive list, yielding high concealing force and whiteness, high compound sturdiness, solid oxidizing power, nontoxicity, ease and accessibility [5–7]. SnO_2–TiO_2 composite exhibits high surface vitality than the individual SnO_2 and TiO_2 [8]. Coupling of TiO_2 with SnO_2 affects the electronic structure and thus facilitates the control and upgrade of the surface concoction and physical properties of the material. Expansion of SnO_2 can improve the photocatalytic movement of TiO_2 can be improved through the expansion of SnO_2, which may be ascribed to the improved charge separation proficiency, and possibly broaden the wavelength scope of photo excitation [9, 10]. Doping of metal oxides or movement of earth metals expands surface imperfections. Improvement of optical and electronic properties is valuable for moving the ingestion of particles toward the apparent locale Tin oxide (SnO_2), a straightforward directing oxide, possesses a tetragonal rutile structure with a band gap of(3.6 eV) [11].

Emptied SnO_2 exhibits low electrical resistance and high optical transparency in the apparent electromagnetic range [12]. This material is utilized as a cathode in sunlight-based cells, light-producing diodes and straightforward electromagnetic protecting materials [13]. In addition, TiO_2 nanostructures exhibit a wide range of potential applications because of their optical and electronic properties [14], which rely on their crystalline state and creation [15]. Solid oxidizing power, high substance dormancy, long-haul security and ease of the titanium dioxide semiconductor permit its utilization in photocatalytic applications. Three conceivable crystalline conditions of TiO_2 are anatase, rutile and brookite. Among these phases, the anatase stage displays the most metastable photocatalytic properties [16].

*Corresponding author e-mail: ali75@uomustansiriyah.edu.iq.; (Ali Mohamad Ali Abdul Amir AL-Mokaram).

Receive Date: 21 March 2021, Revise Date: 04 January 2022, Accept Date: 10 January 2022

DOI: 10.21608/EJCHEM.2022.68381.3503

In numerous applications, TiO_2 displays compelling photochemical properties. Moreover, the material is photo stable, nonselective and non-lethal in the treatment of any harmful natural materials. However, several disadvantages in using TiO_2 include low quantum effectiveness, troublesome division impetus agglomeration. Certain effort has been focused on enhancing the photocatalytic action of TiO_2 in recent years [17].

In general, the dopants presented by the sol–gel technique influence the TiO_2 stage and change the conduct and structure of the material. The effect of dopants on the TiO_2 stage change and grain development before their application intriguing presents intriguing research value [18]. In this paper, we portray the combination of TiO_2 nanoparticles doped with SnO_2 by sol–gel method. The effect of SnO_2 doping on the stage change of TiO_2 anatase or rutile nanostructure was examined, and had improvement particle size, and band gap compared to TiO_2 or SnO_2.

2- Experimental

The chemicals used in this work were of analytical grade and obtained from Merck Chemical Reagent Co. Ltd. Titanium tetra isopropoxide (TTIP), SnO_2 (Sigma-Aldrich), ethanol absolute (Merck) and deionized water were used for preparing the nanoparticle by sol–gel method.

The prepared crystalline nanoparticle structure was characterized by Scanning Electron Microscopy (SEM) (Sigma). The UV–visible absorption spectrum of the nanocrystal was recorded in the wavelength range of (200–800 nm) by using two quartz cells with a (10 mm) pathway in a double-beam spectrophotometer (100 Conc./Varian. USA). The mean particle space was measured through atomic force microscopy (AFM) using an (AA300) scanning probe microscope from Angstrom Advanced Inc. The surface area of the nanoparticle was calculated using an Instrument NOVA station A with nitrogen.

TiO_2 was synthesized from TTIP dissolved in absolute ethanol, and deionized water was added to the solution at a molar ratio of (TTIP: H_2O = 1:4). The solution was added drop wise into a to nitric acid solution under vigorous stirring for hydrolysis of the solution. Then, SnO_2 (0.2 gm) dissolved in absolute ethanol at a molar ratio of (TTIP: SnO_2 = 2:1) was added to the hydrolysis solution under vigorous stirring for (4 h) to form sols. Sols were transformed into gels after (24 h). The gels were dried at (80 °C) for (2 h) to evaporate water and organic material to the maximum extent. Dry gel calcination at (450 °C) for (2 h) was subsequently conducted to obtain the desired TiO_2/SnO_2 nanoparticles as a white powder.

3- Results and Discussion

X-ray diffraction (XRD) technique was used to investigate the phase of the prepared sample. Figure 1 shows the XRD patterns of the prepared sample (TiO_2-coupled SnO_2). The pattern of TiO_2 was indexed to the anatase phase of TiO_2 (JCPDS file No. 21- 1272). This finding is in agreement with previously reported results for pure TiO_2 prepared using the same method.

Figure (1) shows the peaks obtained at 2θ = 25.3°, 37.9°, 48.01°, 53.5° and 55°, with reflection planes (101), (004), (200), (105) and (211), respectively, corresponding to the anatase phase. Tin oxide peaks were obtained at (2θ = 33.9°, 37.8°, 54.07° and 71.27°) with the corresponding reflection planes of (101), (200), (211), and (220). The XRD spectra of the sample of TiO_2/SnO_2 showed high intense peaks of tin oxide and titanium oxides located at (2θ = 25.30°, 26.6°, 33.9° and 53.5°). The peaks become extremely intense in the presence of SnO_2, which may be due to the replacement of tin oxide and titanium oxide atoms.

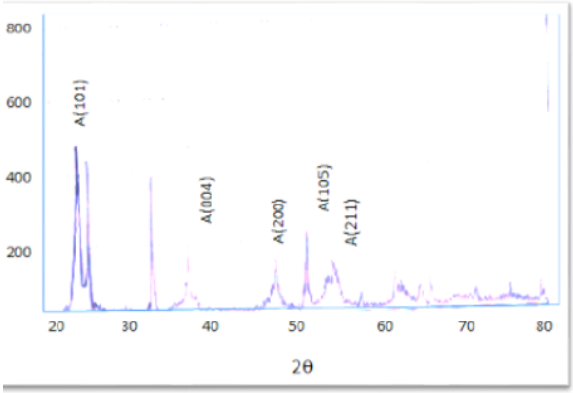

Fig. (1): XRD spectra of TiO_2/SnO_2 nanoparticles.

The anatase phase of titania is affected by dopant nature and concentration; with the amount of dopant in our preparation procedure, minimal Sn +4 content leads to anatase phase formation. Particle size as calculated using Scherrer equation was 26.94 nm.

$D = K\lambda / (B\cos\theta)$….. (1)

Where λ is the wave length of the X-ray, K= 0.89, B is the full- width at have at half maximum peak intensity (FWHM) in radians, D is the diameter of the crystalline and θ is the angle of diffraction.

Muhammad et al. [8] studied influence of gadolinium on SnO_2/TiO_2 nanoparticles and catalytic activity through hydrothermal methods. The group observed that the particle size with gadolinium was (25 nm).

The XRD spectra of Gd/SnO_2–TiO_2 showed peaks of tin and titanium oxides located at (2θ = 25.44°, 27.54°, 37.41°, 51.16°, 58.20°, 68.92° and 44.25°). The coupled system of SnO_2/TiO_2, in which TiO_2 functions as photosensitizer for SnO_2, also attracts considerable interest. Pure SnO_2 shows minimal catalysis because the band gap of SnO_2 (3.5–3.8 eV) was insufficient to initiate photocatalytic reaction. The resulting synthesised nanoparticles chemically showed the surface morphology and size of nanoparticles (Figure 2). The average size of TiO_2/SnO_2 nanoparticles synthesized by sol–gel method was (67 nm). The images show that the synthesized nanoparticles possessed regular shape and uniform morphology. Balachandran et al. [19, 20] showed that colloidal TiO_2 /SiO_2 nanocomposites exhibited regular morphology. The nanoparticles were spherical in shape, and the particle sizes of the nanocomposite was (24 nm).

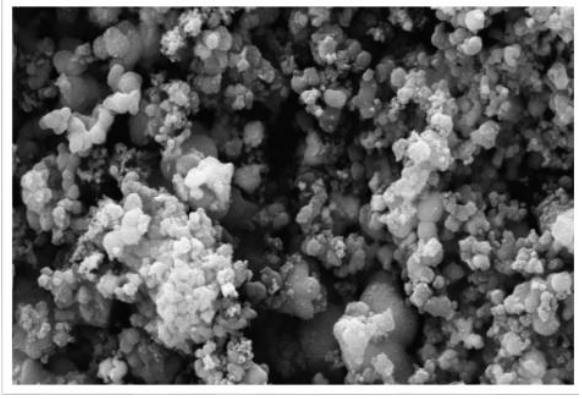

Fig. (2): SEM photographs of the TiO_2/SnO_2 nanoparticles.

Atomic Force microscope (AFM) scans show in figure (3) that the etched surface reverted to the as-grown morphology. The TiO_2 distribution must be concentrated at the surface. Surface adsorbate species was used as a reference; thus, that TiO_2 is limited to the top layers of the surface SnO_2. Figure (3) shows the AFM images of TiO_2/SnO_2.

The surface of TiO_2/SnO_2 nanoparticles exhibited a uniform surface, indicating that additional defects occur under growth condition with orientation distributions. TiO_2/SnO_2 nanoparticles exhibited random orientation with poor degree of crystallinity, and the average diameter of the TiO_2/SnO_2 nanoparticle was (98.99 nm). The root-mean square (RMS) roughness of the nanoparticle can be obtained from AFM analysis.

An RMS of (7.32 nm) was observed on the plain TiO_2/SnO_2 surface. The substantial change in surface roughness matches the analysis results of crystalline growth.

In Figure (4) the FTIR spectrum of SnO_2 shows the localization of the FTIR spectra ranging from (625.89

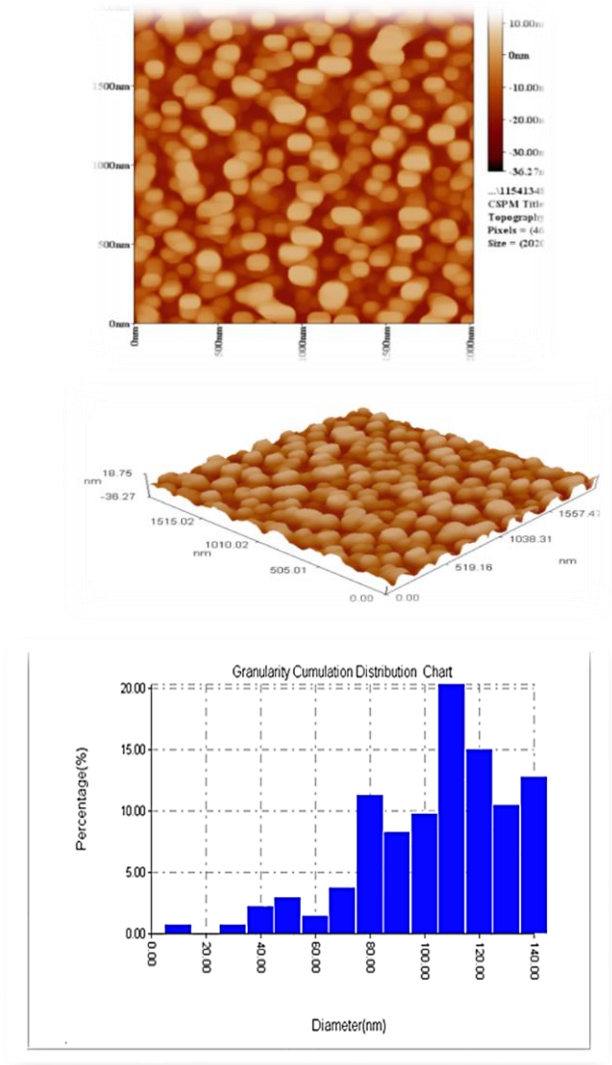

cm^{-1}) to (663.53 cm^{-1}), which corresponds to the vibration of Sn-O band. TiO_2/SnO_2 exhibits the FTIR spectra of a SnO_2- coupled TiO_2 prepared by sol–gel method, with the strong band located at (671.25 cm^{-1}) attributed to Sn–O–Ti bridging stretching modes. The broad band at (3408.33 cm^{-1}) observed in the spectra of coupled sample can be ascribed to surface O–H groups, and the band at (1651.12 cm^{-1}) corresponds to the bending vibrations of O–H and absorbed water molecules. The band at (642.32 cm^{-1}) in spectra was due to Ti–O, which confirms Sn-O bending vibrations at (655.82 cm^{-1}). The assignment of bands in the spectra are listed in Table (1).

Fig. (3): AFM images of TiO_2 / SnO_2 nanoparticles.

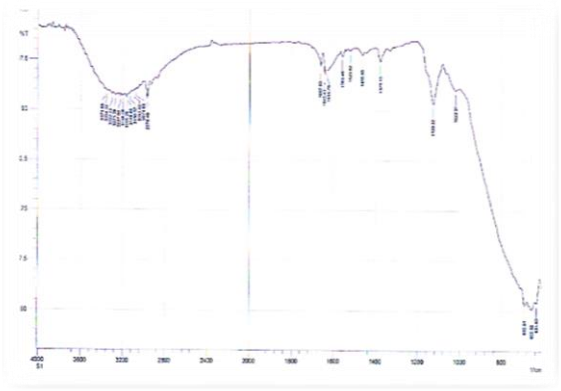

Fig. (4): FTIR spectra of TiO_2/SnO_2 nanoparticles.

Table (1): FTIR data of TiO_2/SnO_2 nanoparticles

Assignment	Wavenumber cm $^{-1}$
O-H	3408.53
Ti-O-Ti	1508.38
Sn-O	663.53 , 625,89, 655.82
Ti-O	642.32
Sn-O-Ti	671.25

In the present work, the band gap for the coupled TiO_2/SnO_2 nanoparticle was approximately (3.69 eV). The response of SnO_2 reduction of the band gap energy enhanced photocatalytic activity towards increased wavelength. The direct band gap of the TiO_2-coupled SnO_2 was determined by the absorption data. The addition of SnO_2 can effectively improve the photocatalytic activity of TiO_2. The preparation of Sn (IV)/TiO_2/activated carbon (AC) by sol–gel method improved the photocatalytic activity of TiO_2, and Sn/TiO_2/AC all exhibited higher catalytic activity than pure TiO_2 /AC [17]. Kinetic study was conducted by analyzing the p-nitro toluene (N.T) removal from aqueous solution at different time intervals.

Heterogeneous photocatalytic reactions show a proportional increase in photo degradation with catalyst loading. However, photonic efficiency diminishes and TiO_2-coupled SnO_2 surface becomes saturated, leading to catalyst deactivation. Different concentrations of the nanoparticles were investigated to select the optimal concentration for efficient photodegradation. As presented in Figure 5 and Table 2, the concentration of TiO_2/SnO_2 (0.075 g L^{-1}) was at approximately (60.7%).

Efficient degradation of p-N.T was achieved in (3 h) at low concentration (1×10^{-4} M). This finding indicates that degradation of p-N.T increases with increasing concentration of TiO_2/SnO_2 until (0.075 g L^{-1}) is reached. By contrast, the efficiency of p-N.T photo degradation is slightly reduced at increased concentration of catalyst. This phenomenon is due to decreased light at a high concentration of the catalyst suspension. Aliwi and Abdul-Kader reported on the photo degradation of propanol in aqueous TiO_2 suspension, which showed that the optimum loading of anatase yielded the highest photodegradation rate of (1.42 g L^{-1}) [22]. concentration for efficient photodegradation. As presented in Figure 5 and Table 2, the concentration of TiO2/SnO2 (0.075 g L−1) was at approximately 60.7%.

Efficient degradation of 4-N.T was achieved in 3 h at low concentration (1×10−4 M). This finding indicates that degradation of 4-N.T increases with increasing concentration of TiO2/SnO2 until 0.075 g L−1 is reached. By contrast, the efficiency of 4-N.T photodegradation is slightly reduced at increased concentration of catalyst. This phenomenon is due to decreased light at a high concentration of the catalyst suspension. Aliwi and Abdul-Kader reported on the photodegradation of propanil in aqueous TiO2 suspension, which showed that the optimum loading of anatase yielded the highest photodegradation rate of 1.42 g L−1 [22].

Table (2) Different loading of nanoparticle TiO_2/ SnO_2, p- N.T (1* 10^{-4} M)

Conc. / t(min)	0.025 g/l	0.075 g/l	0.125 g/l	0.25 g/l
	Ln C_o/C_t	Ln C_o/C_t	Ln C_o/C_t	Ln C_o/C_t
0				
30	0.062	0.155	0.12	0.072
60	0.186	0.290	0.158	0.188
90	0.356	0.340	0.29	0.316
120	0.340	0.550	0.373	0.351
150	0.460	0.707	0.504	0.457
180	0.805	0.936	0.538	0.482

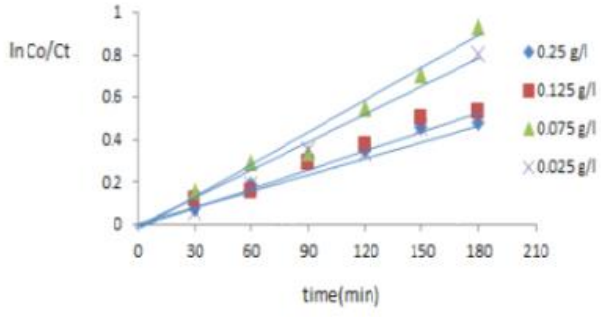

Fig.(5) Different loading of nanoparticle TiO_2 /SnO_2 , p-N.T (1*10^{-4} M)

In the present work, the as-prepared TiO_2-coupled SnO_2 increased the activity of photo catalysis and degradation of p-N.T. Several semiconductors exhibit band gap energies that are suitable for the photocatalytic degradation of contaminants. Among the applied photo catalysts, TiO_2 is one of the most widely used photocatalytic semiconducting materials.

Conc. / t(min)	$1*10^{-4}$ M Ln C_o/C_t	$3*10^{-4}$M Ln C_o/C_t	$5*10^{-4}$M Ln C_o/C_t	$7*10^{-4}$ M Ln C_o/C_t
0				
30	0.155	0.091	0.103	0.094
60	0.29	0.152	0.19	0.215
90	0.34	0.283	0.357	0.444
120	0.55	0.433	0.564	0.701
150	0.707	0.577	0.821	1.045
180	0.936	0.82	1.053	1.183

Furthermore, photo activity is highly dependent on surface area and crystal size, which is consequently influenced by the titania synthetic method. This suggests the pseudo first order kinetics of the primary photolysis process. The decrease in concentration of p-N.T was monitored by following the absorption at 285 nm with different irradiation time, a straight line obtained from the plot of ln (C_o/C_t) versus irradiation time. From the slope of the straight line, the value of the first order specific rate constant (k) was evaluated according to equation (3)

$$\text{Ln}\frac{Co}{Ct} = kt \ldots. (3)$$

. The degradation efficiency of p-N.T increases when the concentration reached a maximum. Photodegradation occurred under the same experimental conditions and was achieved at (180-min) irradiation time. At the initial concentration of p-N.T of (7×10^{-4} M) Figure (6), a high degradation efficiency of (70.6%) was reached at (0.075 g L^{-1}) of TiO_2/SnO_2 loading within the (180 min) irradiation time. The Langmuir–Hinshelwood kinetic formula for this reaction in Figure (7) shows that a straight line obtained from this plot gives slope of adsorption constant (K) value equal to (5×10^2 M^{-1}),the intercept represent the value of rate constant (k)equal (100×10^{-7} $M^{-1}min^{-1}$) respectively, as shown in Table (3).

A decreased concentration of p-N.T from (7×10^{-4} M) resulted in a decrement in degradation efficiency and indicated the difficulty in the adsorption of molecules on the surface of TiO_2/SnO_2. Free-radical production
is limited and thus suppressed the degradation rate. Plot of the reciprocal of the initial rate of p-N.T and nanoparticle TiO_2/SnO_2 (0.075 g L^{-1}) against the inverse of the initial p-N.T concentration.

The effect of the pH value of the starting solution on the size of the TiO_2/SnO_2 nanoparticle was investigated. When pH exceeded (4), TiO_2 /SnO_2 nanoparticle showed serious agglomeration. When the pH increased to (9), the nanoparticle presented poor dispersity and became agglomerated. With the increase in pH value, the concentration of H+ decreases, and the hydroxylation velocity of (Ti^{4+}) is accelerated, resulting in the reunion of (TiO^{2+}) in the solution. TiO_2 is an important photo catalyst for the degradation of organic pollutants in wastewater. Photocatalytic degradation was studied under UV-light. The TiO_2-coupled SnO_2 loading was (0.075 g L^{-1}), and the p- N.T concentration was (7×10^{-4} M). The maximum degradation was obtained at (pH 3) Figure (8); these results were also presented in Table (4). The degradation efficiency was (83.5%)

Table (3) Different concentration of p-N.T, TiO_2/ SnO_2 (0.075 g/l) and pH5.3

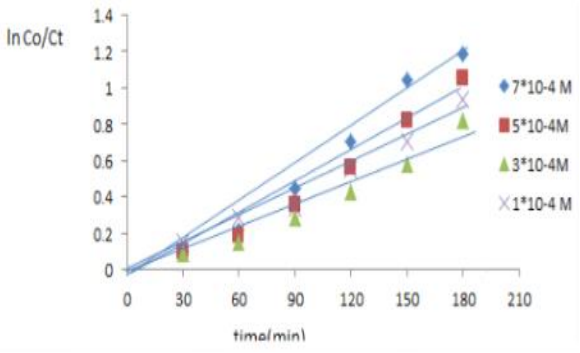

Fig. (6) Different concentration of p-N.T , TiO_2/ SnO_2(0.075 g/l)

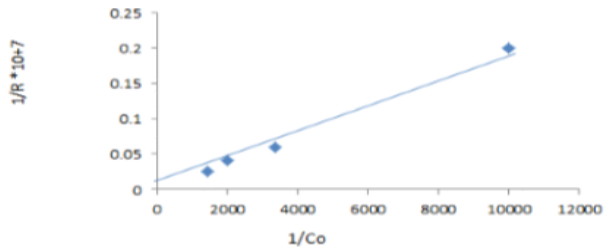

Fig. (7): Plot of the reciprocal of the initial rate of p-N.T, nanoparticle TiO_2/ SnO_2 (0.075 g/l) against the reverse of the initial p- N.T concentration.

Table (4) Different pH for p- N.T ($7*10^{-4}$M), nanoparticle TiO_2/ SnO_2 (0.075 g/l).

pH / t(min)	pH3 Ln C_o/C_t	pH 5.3 Ln C_o/C_t	pH7 Ln C_o/C_t	pH9 Ln C_o/C_t
0				

30	0.087	0.094	0.18	0.102
60	0.437	0.215	0.40	0.198
90	0.703	0.444	0.49	0.40
120	1.017	0.701	0.63	0.535
150	1.360	1.045	0.83	0.807
180	1.837	1.183	0.97	0.90

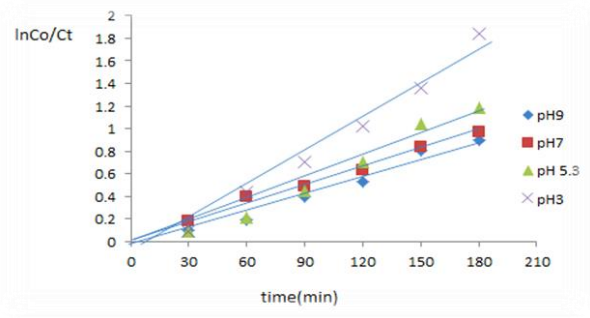

Fig. (8): Different pH for p- N.T (7*10^{-4}M), nanoparticle TiO_2/ SnO_2 (0.075 g/l)

The degradation reaction for p-N.T was investigated by varying the reaction temperature from (288 K to 318 K). Table (5) and Figure (9) show the temperature effect on the decomposition of p- N.T at the initial concentration of (7×10^{-4} M), pH 3, TiO_2/SnO_2 loading of (0.075 g L^{-1})and at (298 K). The rate constant for p-N.T in aqueous TiO_2-coupled SnO_2 suspension at different temperature is shown. At (298 K), a high degradation efficiency (83.5 %) was obtained.

Table (5) Different temperature of nanoparticle nanoparticles TiO_2/ SnO_2 (0.075 g/l), 4-N.T (7*10^{-4}M), pH 3

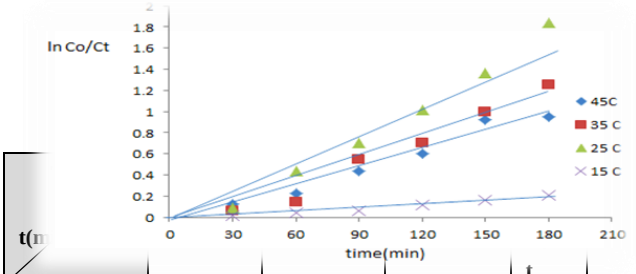

t(min)				t
0				
30	0.014	0.087	0.0576	0.125
60	0.042	0.437	0.141	0.224
90	0.057	0.703	0.55	0.437
120	0.116	1.017	0.706	0.601
150	0.165	1.36	1.00	0.926
180	0.206	1.837	1.25	0.95

Fig. :(9) Different temperature of nanoparticle nanoparticles TiO_2/ SnO_2 (0.075 g/l), 4-N.T (7*10^{-4}M), pH 3

Figure (10) and Table (6) show the Arrhenius plot of the reaction rate constant versus reciprocal of temperature. The activation energy of (29.8979 kJ/mol) was obtained from the slope of the straight line according to Arrhenius equation (2) [24].

$$\ln k = \ln A \quad \frac{-Ea}{RT} \quad \ldots..(2)$$

The photochemical system is generally dependent on temperature; the photocatalytic activity decreases with increasing temperature in the photo degradation of p-N.T by UV irradiation. Thus, the photocatalytic activity of TiO_2-coupled SnO_2 prepared by the sol–gel method is generally temperature independent.

Table (6) Different temperature and rate constant of nanoparticles TiO_2/ SnO_2 (0.075 g/l)

Temp.(°C)	Temp.(°K)	1/ T (K)	Ln K
15	288	0.00347	-6.64
25	298	0.00335	-4.47
35	308	0.00325	-4.71
45	318	0.00314	-3.96

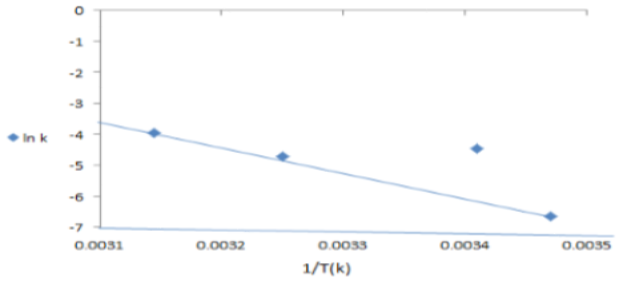

Fig (10) Arrhenius plot for the degradation of p- N.T (7*10^{-4}M) irradiated nanoparticle TiO_2 /SnO_2 (0.075 g/l).

The photocatalytic reaction rate depends largely on the radiation absorption of the photo catalyst. Light scattering in solid–liquid regimes is particularly significant. Therefore, quantum yield is experimentally difficult to determine because metal oxides in a heterogeneous regime, including TiO_2, cannot absorb all of the incident radiation due to refraction. The photo

degradation efficiency of p-N.T was at the maximum under reaction conditions of (pH 3), p-N.T concentration at (7×10^{-4}) and amount of TiO_2/SnO_2 (0.075 g L^{-1}) to ensure the decrease in the concentration of p-N.T by photo degradation in the presence of the photo catalyst TiO_2/SnO_2 under 150W and 300 W (visible light) and sunlight. Photolysis under 300 W reached (86.58%), whereas that under UV- light reached (83.5%).The (86.58%) and (83.5%) photo degradation were achieved under 150 W and sunlight irradiation within (180 min). The results are shown in Figures (11, 12) and Tables (7, 8).

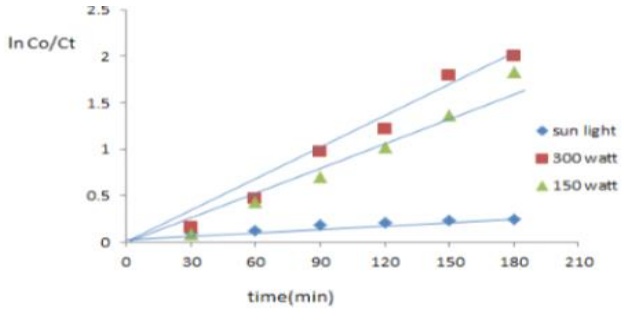

Fig. (11) Different light sources for p- N.T ($7*10^{-4}$ M), nanoparticles TiO_2 /SnO_2 (0.075 g/ l) and pH 3

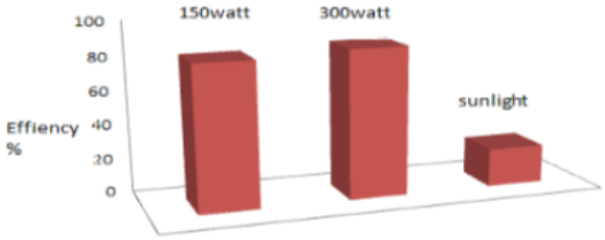

Fig. (12) Efficiency of sources light of degradation of p-N.T

Table (7) Different light sources for p- N.T ($7*10^{-4}$ M), nanoparticle TiO_2 /SnO_2 (0. 075 g/ l) and pH 3.

Source / T(min)	150 watt	300 watt	sun light
	Ln C_o/C_t	Ln C_o/C_t	Ln C_o/C_t
0			
30	0.087	0.165	0.0947
60	0.437	0.466	0.125
90	0.703	0.97	0.1906
120	1.017	1.216	0.216
150	1.36	1.798	0.233
180	1.837	2.01	0.253

Table (8) the results of TiO_2 / SnO_2 nanoparticle of photo degradation of p- NT

Conc.of nanoparticle(g/l)	Efficiency%	K (min^{-1}) $*10^{-3}$	Rate$(Mmin^{-1})*10^{-7}$
0.025	56	4.3	4.3
0.075	60.7	5.0	5.0
0.175	41.7	3.1	3.1
0.25	38.6	2.8	2.8
Conc. of p-Nitrotolune (M)$*10^{-4}$	Efficiency%	K (min^{-1}) $*10^{-3}$	Rate$(Mmin^{-1})*10^{-7}$
1	60.7	5.0	5.0
3	63.0	5.6	16.8
5	65.2	6.5	32.5
7	70.6	7.8	54.6
pH	Efficiency%	K (min^{-1}) $*10^{-3}$	Rate$(Mmin^{-1})*10^{-7}$
3	83.5	11.4	79.8
4.6	70.6	7.8	54.6
7	62.3	5.1	35.7
9	59.4	5.7	39.9
Temp. °C	Efficiency%	K (min^{-1}) $*10^{-3}$	Rate$(Mmin^{-1})*10^{-7}$
15	18.5	1.3	9.1
25	83.5	11.4	79.8
35	74.6	9.0	63.0
45	71.4	7.5	52.5
Sources (watt)	Efficiency%	K (min^{-1}) $*10^{-3}$	Rate$(Mmin^{-1})*10^{-7}$
150	83.5	11.4	79.8
300	86.58	13.0	91.0
Sun light	22.4	11.0	7.7

4-Conclusion

TiO_2/SnO_2 nanoparticles were integrated through sol–gel technique. The expansion of SnO_2 in the nanoparticle creation strategy caused vital changes to the surface. X-ray diffraction estimation revealed the TiO_2/SnO_2 molecule size was 26.94 nm.. SEM images demonstrated the development of round moulded nanoparticles. Pore volume and surface territory markedly decreased compared with that of the unadulterated titanium dioxide. The band gap of TiO_2/SnO_2 was 3.69 eV. The TiO_2/SnO_2 nanoparticles prepared by sol–gel method displayed moderately high photocatalytic proficiency in the photograph degeneration of p-N.T. The photocatalytic activities for the TiO_2 coupled SnO_2 investigated as evaluated by photo degradation of p-NT solution were found to depend on the kind of dopant introduced into TiO_2 lattice, and showed the highest rate constant and the highest efficiency .High photocatalytic efficiency was observed with a medium pH 3. The photodegeneration of p-nitrotoleune at a TiO_2/SnO_2 nanoparticle concentration of (0.075 g $L^{-1)}$ by 300 W yielded a p-N.T deterioration of up to 86.58% in the presence of the photocatalyst, less concentration of p-N.T from (7×10^{-4} M) resulted in a decrement in degradation

efficiency that indicated the difficulty in the adsorption of molecules on the surface of TiO_2/SnO_2. Photolysis under 300 watt was efficiency% (86.58%), whereas efficiency% by used UV- light reached (83.5%).As well that photocatalytic activity decreases with increasing temperature, the activation energy of (29.8979 kJ/mol.) was obtained .

5-Acknowledgement

The Authors would like to thanks the Department of Chemistry at the College of Science – Mustansiriyah University for their technancial support. https://uomustansiriyah.edu.iq/

6-References

1-Karuppuchamy, S. and Jeong, J.M. Synthesis of nano-particles of TiO_2 by simple aqueous route. *Journal of Oleo Science*, 55(5), pp.263-266 (2006).

2- Sanda, M.D.A., Badu, M., Awudza, J.A. and Boadi, N.O. Development of TiO_2-based dye-sensitized solar cells using natural dyes extracted from some plant-based materials. *Chem Int*, *7*(1), pp.9-20(2021).

3-Mingxue, B., Shunya, N., Kaho, Y., and Naofumi, O. Photocatalytic Performance of an Anodic TiO_2 Layer Fabricated in a NH4NO3/Ethylene Glycol Electrolyte with Various Crystallographic Phases. *MATERIALS TRANSACTIONS.* 60:9, 1821-18279 (2019).

4-Chi, Y.H., Pravinraj, S., Govindan, S. and Che J.H. Electro-optical and dielectric properties of TiO_2 nanoparticles in nematic liquid crystals with high dielectric anisotropy.*Journal of Molecular Liquids*,286,110902, (2019).

5- Katal, R., Masudy-Panah, S., Tanhaei, M., Farahani, M.H.D.A. and Jiangyong, H.. A review on the synthesis of the various types of anatase TiO_2 facets and their applications for photocatalysis. *Chemical Engineering Journal*, *384*, p.123384 (2020).

6- Pawar, M., Topcu Sendoğdular, S. and Gouma, P. A brief overview of TiO_2 photocatalyst for organic dye remediation: case study of reaction mechanisms involved in Ce-TiO2 photocatalysts system. *Journal of Nanomaterials*, *2018*.

7-Al-Mokaram, A., Amir, M.A., Yahya, R., Abdi, M.M. and Mahmud, H.N.M.E. The development of non-enzymatic glucose biosensors based on electrochemically prepared polypyrrole–chitosan–titanium dioxide nanocomposite films. Nanomaterials, 7(6), p.129.(2017).

8-Khaleeq-ur-Rahman, M.,.Muhammad Akhyar Farrukh, Maryam Shahid, Iqra Muneer, and Shaghraf Javaid . *J Mater Sci: Mater Electron*, *27*, pp.2994-3002(2016).

9- Beltran, A., Andres, J., Sambrano, J.R. and Longo, E. Density functional theory study on the structural and electronic properties of low index rutile surfaces for $TiO_2/SnO_2/TiO_2$ and $SnO_2/TiO_2/SnO_2$ composite systems. *The Journal of Physical Chemistry A*, *112*(38), pp.8943-8952(2008).

10-Labat, F., Baranek, P. and Adamo, C. Structural and electronic properties of selected rutile and anatase TiO_2 surfaces: an ab initio investigation. *Journal of Chemical Theory and Computation*, *4*(2), pp.341-352. (2008)

11- Perveen, H., Farrukh, M.A., Khaleeq-ur-Rahman, M., Munir, B. and Tahir, M.A. Synthesis, structural properties and catalytic activity of MgO-SnO_2 nanocatalysts. *Russian Journal of Physical Chemistry A*, *89*(1), pp.99-107. (2015).

12- Javaid, S., Farrukh, M.A., Muneer, I., Shahid, M., Khaleeq-ur-Rahman, M. and Umar, A.A. Influence of optical band gap and particle size on the catalytic properties of Sm/SnO_2–TiO_2 nanoparticles. *Superlattices and Microstructures*, *82*, pp.234-247 (2015).

13- Manifacier, J.C., De Murcia, M., Fillard, J.P. and Vicario, E.. Optical and electrical properties of SnO_2 thin films in relation to their stoichiometric deviation and their crystalline structure. *Thin solid films*, *41*(2), pp.127-135 (1997).

14-Reddy, K.M., Manorama, S.V. and Reddy, A.R. Bandgap studies on anatase titanium dioxide nanoparticles. *Materials Chemistry and Physics*, *78*(1), pp.239-245(2002).

15-Jing, L., Li, S., Song, S., Xue, L. and Fu, H. Investigation on the electron transfer between anatase and rutile in nano-sized TiO2 by means of surface photovoltage technique and its effects on the photocatalytic activity. *Solar Energy Materials and Solar Cells*, *92*(9), pp.1030-1036 (2008).

16- Wang, G. Hydrothermal synthesis and photocatalytic activity of nanocrystalline TiO_2 powders in ethanol–water mixed solutions. *Journal of Molecular Catalysis A: Chemical*, 274(1-2), pp.185-191 (2007).

17-Sun, J., Wang, X., Sun, J., Sun, R., Sun, S. and Qiao, L. Photocatalytic degradation and kinetics of Orange G using nano-sized Sn (IV)/TiO_2/AC photocatalyst. *Journal of molecular catalysis A: Chemical*, *260*(1-2), pp.241-246. (2006).

18-Naser, E., 2, AL-Mokaram A., and Hussein F. Characterization and Applications of Innovative Sn-doped TiO_2/AC and PPy-CS/Sn-doped

TiO_2Nanocomposites as Adsorbent Materials. *Pollution*, 7(2): 445-456 (2021) (in press).

19- Balachandran, K., Venckatesh, R. and Sivaraj, R. Synthesis of nano TiO_2-SiO_2 composite using sol–gel method: effect on size, surface morphology and thermal stability 3695-3695. (2010).

20-Balachandran, K., Venckatesh R. and Sivaraj, R. Photocatalytic decomposition of isolan black by TiO_2 , TiO_2- SiO_2 Core shell nanocomposites)International *J. of Research in Engineering and Technology* , Vol 2, p46-51(2013).

21- Khairy, M. and Zakaria, W. Effect of metal-doping of TiO_2 nanoparticles on their photocatalytic activities toward removal of organic dyes. *Egyptian Journal of Petroleum*, *23*(4), pp.419-426 (2014).

22-Konstantinou, I.K., Sakkas, V.A. and Albanis, T.A.. Photocatalytic degradation of the herbicides propanil and molinate over aqueous TiO2 suspensions: identification of intermediates and the reaction pathway. *Applied Catalysis B: Environmental*, *34*(3), pp.227-239(2000).

23- A.Mehrizad, P.Gharbani, S.M. Tabatabii(Synthesis of Nano sized TiO_2 powder by Sol- Gel method in acidic conditions) J. Iran .Chem..Res.. 2, p 145-149, 2009.

24-V.H.Carvalho, N.D.Coutinho,V.Aquilanti (Temperature Dependence of Rate Processes Beyond Arrhenius and Eyring: Activation and Transitivity) Front. Chem, 2019.